Available online at www.sciencedirect.com
ScienceDirect
Applied Mathematics and Computation 186 (2007) 159–174
APPLIED MATHEMATICS AND COMPUTATION
www.elsevier.com/locate/amc

# Remarks on the Kalman filtering simulation and verification

Dah-Jing Jwo

*Department of Communications and Guidance Engineering, National Taiwan Ocean University, 2 Peining Rd., Keelung 202, Taiwan, ROC*

**Abstract**

The purpose of this paper is to convey the readers several useful remarks for understanding, simulating and verifying the Kalman filter (KF) computer codes. A tutorial, example-based approach is employed to present several KF issues of considerable importance in engineering practice, and to suggest some check points on Kalman filtering verification process. Some illustrative examples are accompanied where necessary to the readers for better understanding the fundamental basis and for enhancing the reliability (correctness) of the self-developed computer codes before larger, complicated KF designs are performed. Notes on two forms of discrete-time Kalman filter loop are pointed out. Methods for determining the process noise covariance matrix are provided. Simulation of the dynamic process is discussed. Guidelines for verification of filtering solutions are provided, which cover (1) the consistency check between the discrete-time to the continuous-time covariance and gain matrices; (2) evaluation of estimator optimality with sensitivity analysis and consistency check between theoretical and simulation results.


*Keywords:* Kalman filter; Simulation; Verification; Optimality evaluation; Sensitivity analysis

## 1. Introduction

The Kalman filter [1–6] (KF) or its nonlinear version, extended Kalman filter (EKF), has been the most well known sequential data assimilation scheme for solving the Wiener problem in a generally easier way. It has been applied in the areas as diverse as aerospace, marine navigation, radar target tracking, control systems, manufacturing, and many others. For the aerospace navigation applications, it has been very popular in GPS/INS and GPS stand-alone navigation designs and is recognised as the navigation's integration workhorse. A navigation filter is commonly designed by use of a Kalman filter to estimate the vehicle state variables and suppress the navigation measurement noise. The Kalman filter not only works well in practice, but also it is theoretically attractive because it has been shown that it is the filter that minimizes the variance of the estimation mean square error.

Studying the operation of the Kalman filter leads to an appreciation of the inter-disciplinary nature of system engineering. However, implementation of the Kalman filter is a challenge to some system designers. A

*E-mail address:* djjwo@mail.ntou.edu.tw

0096-3003/$ - see front matter 
doi:10.1016/j.amc.2006.06.124

deeper understanding of the theory and awareness of practical implementation can only be experienced by employing the filter in practical situation. It may not be such a difficult task to develop a KF computer code. However, it is a challenge to assure its reliability. Even after constructing the program code, some designers may not be able to ensure the correctness of the computer code developed by them. Based on the consideration, several practical remarks are pointed out in this article for clarifying some fundamental concept and conveying some important phenomena. For better illustration, numerical examples are provided where necessary to the readers for better understanding the fundamental basis. The remarks presented in this paper are beneficial to the KF designers, which can be employed as guidelines for developing reliable Kalman filter computer codes.

This paper is organized as follows. In Section 2, additional notes on discrete-time Kalman filter (DTKF) loop are pointed out. In Section 3, determination of the process noise covariance matrix is presented. Simulation of the dynamic process is discussed in Section 4. In Section 5, relation of the DTKF to the continuous Kalman filter (CKF) is shown. The evaluation of estimator optimality for verification of minimum variance optimality with sensitivity analysis and consistency check is provided in Section 6. The conclusion is given in Section 7.

## 2. Additional notes on discrete-time Kalman filter loop

Consider a dynamical system whose state is described by a linear, vector differential equation. The process model and measurement model are represented as

$$\text{Process model}: \dot{\mathbf{x}} = \mathbf{F}\mathbf{x} + \mathbf{G}\mathbf{u}, \tag{1}$$

$$\text{Measurement model}: \mathbf{z} = \mathbf{H}\mathbf{x} + \mathbf{v}, \tag{2}$$

where the vectors $\mathbf{u}(t)$ and $\mathbf{v}(t)$ are both white noise sequences with zero means and mutually independent:

$$E[\mathbf{u}(t)\mathbf{u}^{\mathrm{T}}(\tau)] = \mathbf{Q}\delta(t-\tau), \tag{3a}$$

$$E[\mathbf{G}(t)\mathbf{u}(t)(\mathbf{G}(t)\mathbf{u}(\tau))^{\mathrm{T}}] = \mathbf{G}\mathbf{Q}\mathbf{G}^{\mathrm{T}}\delta(t-\tau), \tag{3b}$$

$$E[\mathbf{v}(t)\mathbf{v}^{\mathrm{T}}(\tau)] = \mathbf{R}\delta(t-\tau), \tag{4}$$

$$E[\mathbf{u}(t)\mathbf{v}^{\mathrm{T}}(\tau)] = \mathbf{0}, \tag{5}$$

where $\delta(t-\tau)$ is the Dirac delta function, $E[\cdot]$ represents expectation, and superscript "T" denotes matrix transpose.

### 2.1. The continuous Kalman filter

The state estimate equation of the continuous Kalman filter equations is represented as

$$\dot{\hat{\mathbf{x}}} = \mathbf{F}\mathbf{x} + \mathbf{K}(\mathbf{z} - \mathbf{H}\hat{\mathbf{x}}). \tag{6}$$

The propagation of the error for a continuous Kalman filter can be described by the Riccati equation,

$$\dot{\mathbf{P}} = \mathbf{F}\mathbf{P} + \mathbf{P}\mathbf{F}^{\mathrm{T}} - \mathbf{P}\mathbf{H}^{\mathrm{T}}\mathbf{R}^{-1}\mathbf{H}\mathbf{P} + \mathbf{G}\mathbf{Q}\mathbf{G}^{\mathrm{T}} \tag{7}$$

and the continuous filter gain is obtained through the calculation

$$\mathbf{K} = \mathbf{P}\mathbf{H}^{\mathrm{T}}\mathbf{R}^{-1}. \tag{8}$$

The discrete filter gain and continuous filter gain are related by

$$\mathbf{K} = \frac{\mathbf{K}_k}{\Delta t}, \tag{9}$$

where $\Delta t = t_{k+1} - t_k$ represents the sampling period. When the system reaches steady-state, $\dot{\mathbf{P}} = \mathbf{0}$, Eq. (7) becomes an Algebraic Riccati Equation (ARE), which can be solved for the steady-state minimum covariance matrix.

### 2.2. Two forms of discrete time Kalman filter loop

Expressing Eqs. (1) and (2) in discrete-time equivalent form via discretisation of a continuous time system leads to

$$\mathbf{x}(t_{k+1}) = \mathbf{\Phi}(t_{k+1}, t_k)\mathbf{x}(t_k) + \int_{t_k}^{t_{k+1}} \mathbf{\Phi}(t_{k+1}, \tau)\mathbf{G}(\tau)\mathbf{u}(\tau)\,\mathrm{d}\tau \tag{10}$$

for which either two of the following abbreviated notations can be used:

$$\mathbf{x}_{k+1} = \mathbf{\Phi}_k\mathbf{x}_k + \mathbf{w}_k, \tag{11a}$$

$$\mathbf{x}_{k+1} = \mathbf{\Phi}_k\mathbf{x}_k + \mathbf{\Gamma}_k\mathbf{w}_k, \tag{11b}$$

$$\mathbf{z}_k = \mathbf{H}_k\mathbf{x}_k + \mathbf{v}_k. \tag{12}$$

In the above equation, the state vector $\mathbf{x}_k \in \Re^n$, process noise vector $\mathbf{w}_k \in \Re^n$, measurement vector $\mathbf{z}_k \in \Re^m$, and measurement noise vector $\mathbf{v}_k \in \Re^m$. Eq. (11b) can be treated as a special case of (11a) for $\mathbf{\Gamma}_k = \mathbf{I}$. In Eqs. (11) and (12), both the vectors $\mathbf{w}_k$ and $\mathbf{v}_k$ are zero mean Gaussian white sequences having zero cross-correlation with each other:

$$\mathbf{E}[\mathbf{w}_k\mathbf{w}_i^{\mathrm{T}}] = \mathbf{Q}_k\delta_{ik} \tag{13a}$$

or alternatively

$$\mathbf{E}[(\mathbf{\Gamma}_k\mathbf{w}_k)(\mathbf{\Gamma}_i\mathbf{w}_i)^{\mathrm{T}}] = \mathbf{\Gamma}_k\mathbf{Q}_k\mathbf{\Gamma}_k\delta_{ik}, \tag{13b}$$

$$\mathbf{E}[\mathbf{v}_k\mathbf{v}_i^{\mathrm{T}}] = \mathbf{R}_k\delta_{ik}, \tag{14}$$

$$\mathbf{E}[\mathbf{w}_k\mathbf{v}_i^{\mathrm{T}}] = \mathbf{0} \quad \text{for all } i \text{ and } k, \tag{15}$$

where $\mathbf{Q}_k$ is the process noise covariance matrix, $\mathbf{R}_k$ is the measurement noise covariance matrix, and $\mathbf{\Phi}_k$ is the state transition matrix. The symbol $\delta_{ik}$ stands for the Kronecker delta function:

$$\delta_{ik} = \begin{cases} 1, & i = k, \\ 0, & i \neq k. \end{cases}$$

Two forms of the discrete-time Kalman filter loop are summarized as follow.

(1) Five-step recursive loop
The five-step recursive loop algorithm iteratively applies two stages of computations [3]:
Stage 1: prediction steps/time update equations

$$\hat{\mathbf{x}}_{k+1}^- = \mathbf{\Phi}_k\hat{\mathbf{x}}_k, \tag{16}$$

$$\mathbf{P}_{k+1}^- = \mathbf{\Phi}_k\mathbf{P}_k\mathbf{\Phi}_k^{\mathrm{T}} + \mathbf{Q}_k. \tag{17a}$$

Stage 2: correction steps/measurement update equations

$$\mathbf{K}_k = \mathbf{P}_k^-\mathbf{H}_k^{\mathrm{T}}[\mathbf{H}_k\mathbf{P}_k^-\mathbf{H}_k^{\mathrm{T}} + \mathbf{R}_k]^{-1}, \tag{18}$$

$$\hat{\mathbf{x}}_k = \hat{\mathbf{x}}_k^- + \mathbf{K}_k[\mathbf{z}_k - \mathbf{H}_k\hat{\mathbf{x}}_k^-], \tag{19}$$

$$\mathbf{P}_k = [\mathbf{I} - \mathbf{K}_k\mathbf{H}_k]\mathbf{P}_k^-. \tag{20}$$

If Eq. (11b) is used, Eq. (17b) should be use to replace Eq. (17a):

$$\mathbf{P}_{k+1}^- = \mathbf{\Phi}_k\mathbf{P}_k\mathbf{\Phi}_k^{\mathrm{T}} + \mathbf{\Gamma}_k\mathbf{Q}_k\mathbf{\Gamma}_k^{\mathrm{T}}. \tag{17b}$$

Eqs. (16)–(20) constitute the Kalman filter for the model of Eqs. (11) and (12). Eqs. (16) and (17) are the time update equations of the algorithm from $k$ to step $k+1$, and Eqs. (18)–(20) are the measurement update equations. These equations incorporate a measurement value into a priori estimation to obtain an improved a posteriori estimation. In the above equations, $\mathbf{P}_k$ is the error covariance matrix defined by $E[(\mathbf{x}_k - \hat{\mathbf{x}}_k)(\mathbf{x}_k - \hat{\mathbf{x}}_k)^{\mathrm{T}}]$, in which $\hat{\mathbf{x}}_k$ is an estimation of the system state vector $\mathbf{x}_k$, and the weighting

matrix $\mathbf{K}_k$ is called the Kalman gain matrix. The Kalman filter algorithm starts with an initial condition value, $\hat{\mathbf{x}}_0^-$ and $\mathbf{P}_0^-$. When new measurement $\mathbf{z}_k$ becomes available with the progression of time, the estimation of states and the corresponding error covariance would follow recursively ad infinity. The difference $(\mathbf{z}_k - \mathbf{H}_k\hat{\mathbf{x}}_k^-)$ in Eq. (19) is generally referred to as the measurement innovation, or the residual. The innovation reflects the discrepancy between the predicted measurement $\mathbf{H}_k\hat{\mathbf{x}}_k^-$ and the actual measurement $\mathbf{z}_k$. An innovation of zero means that the two are in complete agreement. The mean of the corresponding error of an unbiased estimator is zero.

(2) Three-step recursive loop
The alternative loop which only has three steps is summarized as follows:

$$\mathbf{K}_k = \mathbf{P}_k^-\mathbf{H}_k^{\mathrm{T}}[\mathbf{H}_k\mathbf{P}_k^-\mathbf{H}_k^{\mathrm{T}} + \mathbf{R}_k]^{-1}, \tag{21}$$

$$\hat{\mathbf{x}}_k = \mathbf{\Phi}_k\hat{\mathbf{x}}_k + \mathbf{K}_k[\mathbf{z}_k - \mathbf{H}_k\mathbf{\Phi}_k\hat{\mathbf{x}}_k], \tag{22}$$

$$\mathbf{P}_{k+1}^- = \mathbf{\Phi}_k[\mathbf{I} - \mathbf{K}_k\mathbf{H}_k]\mathbf{P}_k^-\mathbf{\Phi}_k^{\mathrm{T}} + \mathbf{Q}_k \tag{23a}$$

which, when represented by Eq. (11b), has the alternative representation form:

$$\mathbf{P}_{k+1}^- = \mathbf{\Phi}_k[\mathbf{I} - \mathbf{K}_k\mathbf{H}_k]\mathbf{P}_k^-\mathbf{\Phi}_k^{\mathrm{T}} + \mathbf{\Gamma}_k\mathbf{Q}_k\mathbf{\Gamma}_k^{\mathrm{T}}. \tag{23b}$$

Eq. (22) can be seen as the combination of Eqs. (16) and (19); while Eq. (23) can be seen as the combination of Eqs. (17) and (20). It should be noted that only the predicted (a priori) covariance is available during the recursive loop; the updated (a posteriori) covariance information does not appear explicitly.

## 3. Determination of the process noise covariance matrix

The matrices $\mathbf{Q}(t)$ – the power spectral density (PSD) matrix, and $\mathbf{Q}_k$ – the covariance matrix are different. There is an important distinction between the matrices $\mathbf{Q}(t)$ and $\mathbf{Q}_k$. A PSD matrix may be converted to a covariance matrix through multiplication by the Dirac delta function, $\delta(t-\tau)$, which has the units of 1/time. Determination of the process noise covariance matrix is discussed mainly based on the assumption that the forcing function is treated either random or deterministic.

### 3.1. Fundamental background

(1) Approach 1: Treat the forcing function as random
This approach is based on the continuous-time white noise approximation. Using the Taylor's series expansion, the state transition matrix can be represented as

$$\mathbf{\Phi}_k = \mathrm{e}^{\mathbf{F}\Delta t} = \mathbf{I} + \mathbf{F}\Delta t + \frac{\mathbf{F}^2\Delta t^2}{2!} + \frac{\mathbf{F}^3\Delta t^3}{3!} + \cdots \tag{24}$$

For the process model given by Eq. (11b), the noise input is given by

$$\mathbf{\Gamma}_k\mathbf{w}_k = \int_{t_k}^{t_{k+1}} \mathbf{\Phi}(t_{k+1},\tau)\mathbf{G}(\tau)\mathbf{u}(\tau)\,\mathrm{d}\tau, \tag{25}$$

where we defined $t_k \equiv k\Delta t$ and $t_{k+1} \equiv (k+1)\Delta t$, and the calculation of process noise covariance, as defined in Eq. (13b) leads to

$$\begin{aligned}\mathbf{\Gamma}_k\mathbf{Q}_k\mathbf{\Gamma}_k^{\mathrm{T}} &= E[(\mathbf{\Gamma}_k\mathbf{w}_k)(\mathbf{\Gamma}_k\mathbf{w}_k)^{\mathrm{T}}] = E\left\{\left[\int_{t_k}^{t_{k+1}} \mathbf{\Phi}(t_{k+1},\xi)\mathbf{G}(\xi)\mathbf{u}(\xi)d\xi\right]\left[\int_{t_k}^{t_{k+1}} \mathbf{\Phi}(t_{k+1},\eta)\mathbf{G}(\eta)\mathbf{u}(\eta)\,\mathrm{d}\eta\right]^{\mathrm{T}}\right\} \\ &= \int_{t_k}^{t_{k+1}}\int_{t_k}^{t_{k+1}} \mathbf{\Phi}(t_{k+1},\xi)\mathbf{G}(\xi)E[\mathbf{u}(\xi)\mathbf{u}^{\mathrm{T}}(\eta)]\mathbf{G}^{\mathrm{T}}\mathbf{\Phi}^{\mathrm{T}}(t_{k+1},\eta)d\xi\,\mathrm{d}\eta \\ &= \int_{t_k}^{t_{k+1}} \mathbf{\Phi}(t_{k+1},\eta)\mathbf{G}\mathbf{Q}\mathbf{G}^{\mathrm{T}}\mathbf{\Phi}^{\mathrm{T}}(t_{k+1},\eta)\,\mathrm{d}\eta.\end{aligned} \tag{26}$$

It is seen that when $\mathbf{\Phi}_k \approx \mathbf{I}$, the first-order approximation is

$$\mathbf{\Gamma}_k \mathbf{Q}_k \mathbf{\Gamma}_k^{\mathrm{T}} \approx \mathbf{G}\mathbf{Q}\mathbf{G}^{\mathrm{T}} \Delta t. \tag{27}$$

The expression when including the higher order terms is given by

$$\mathbf{\Gamma}_k \mathbf{Q}_k \mathbf{\Gamma}_k^{\mathrm{T}} = \mathbf{G}\mathbf{Q}\mathbf{G}^{\mathrm{T}} \Delta t + \frac{(\mathbf{F}\mathbf{G}\mathbf{Q}\mathbf{G}^{\mathrm{T}} + \mathbf{G}\mathbf{Q}\mathbf{G}^{\mathrm{T}}\mathbf{F}^{\mathrm{T}})\Delta t^2}{2!} + \cdots$$

On the other hand, for the process model given by Eq. (11a), the noise input is then given by

$$\mathbf{w}_k = \int_{t_k}^{t_{k+1}} \mathbf{\Phi}(t_{k+1}, \tau)\mathbf{G}(\tau)\mathbf{u}(\tau)\,\mathrm{d}\tau$$

and the covariance of the process noise, $\mathbf{w}_k$, as defined in Eq. (13a) leads to

$$\mathbf{Q}_k = E[\mathbf{w}_k \mathbf{w}_i^{\mathrm{T}}] = \int_{t_k}^{t_{k+1}} \mathbf{\Phi}(t_{k+1}, \eta)\mathbf{G}\mathbf{Q}\mathbf{G}^{\mathrm{T}}\mathbf{\Phi}^{\mathrm{T}}(t_{k+1}, \eta)\,\mathrm{d}\eta \tag{28}$$

and when $\mathbf{\Phi}_k \approx \mathbf{I}$

$$\mathbf{Q}_k \approx \mathbf{G}\mathbf{Q}\mathbf{G}^{\mathbf{T}} \Delta t. \tag{29}$$

Eq. (29) can be regarded as a special case of Eq. (27) where the noise gain is set as an identity matrix: $\mathbf{\Gamma}_k = \mathbf{I}$. For a complete description of the influence by the random forcing functions, the term $\mathbf{\Gamma}_k \mathbf{Q}_k \mathbf{\Gamma}_k^{\mathrm{T}}$ should be used and the relation $\mathbf{\Gamma}_k \mathbf{Q}_k \mathbf{\Gamma}_k^{\mathrm{T}} \approx \mathbf{G}\mathbf{Q}\mathbf{G}^{\mathrm{T}} \Delta t$ always holds valid for both types of representation.

(2) Approach 2: Treat the forcing function as deterministic

This approach is based on the piecewise white noise or discrete white noise approximation. Assuming that the forcing function $\mathbf{u}(\tau)$ has a constant value of $\mathbf{u}(t) = \mathbf{w}_k$ over the integration interval, i.e., for $t \in [t_k, t_{k+1}]$ for all $k = 0,1,2,\ldots,$ then the noise gain

$$\mathbf{\Gamma}_k = \int_{t_k}^{t_{k+1}} \mathbf{\Phi}_k(t_{k+1}, \tau)\mathbf{G}(\tau)\,\mathrm{d}\tau. \tag{30}$$

Eq. (30) can be written as the following series expansion:

$$\mathbf{\Gamma}_k = \mathbf{G}\Delta t + \frac{\mathbf{F}\mathbf{G}\Delta t^2}{2!} + \cdots \tag{31}$$

Hence, for the first-order approximation, we have $\mathbf{\Gamma}_k \approx \mathbf{G}\Delta t$ when $\mathbf{\Phi}_k \approx \mathbf{I}$ (which is equivalently to $\mathbf{F} = \mathbf{0}$), and

$$\mathbf{\Gamma}_k \mathbf{Q}_k \mathbf{\Gamma}_k^{\mathrm{T}} \approx (\mathbf{G}\Delta t)\mathbf{Q}_k(\mathbf{G}\Delta t)^{\mathrm{T}}. \tag{32}$$

Equating Eqs. (32) and (27) gives

$$\mathbf{Q}_k \approx \frac{\mathbf{Q}}{\Delta t}. \tag{33}$$

Note the difference between Eqs. (33) and (29). It is important that $\mathbf{Q}_k$'s ingredients in the two equations are different.

### 3.2. Illustrative example

For the sake of better illustration, the radar target tracking in one dimension is employed in this and also the following sections where applicable. When modelling for a vehicle kinematics, the positions at $t_k$ and $t_{k+1}$ may be related by

$$p_{k+1} = p_k + \dot{p}_k \Delta t + \ddot{p}_k \frac{\Delta t^2}{2!} + \dddot{p}_k \frac{\Delta t^3}{3!} + \cdots,$$

where the number of dots indicates the order of differentiation. The model is approximated by a truncated series, either using a constant velocity model:

$$p_{k+1} = p_k + \dot{p}_k \Delta t \tag{34}$$

or a constant acceleration model:

$$p_{i+1} = p_i + \dot{p}_i \Delta t + \ddot{p}_i \frac{\Delta t^2}{2!}, \tag{35}$$

where $p_i$ and $\dot{p}_i$ of Eqs. (34) and (35) are considered constant for the time interval $\Delta t$, and $\ddot{p}_k$ of Eq. (35) is considered constant for the time interval $\Delta t$. The validity of these assumptions is dependent on the length of $\Delta t$ and the degree of the linearity of the vehicle's motion. The differential equation of the observed system ca be represented either of the following forms:

$$\frac{\mathrm{d}}{\mathrm{d}t}\begin{bmatrix} x_1 \\ x_2 \end{bmatrix} = \begin{bmatrix} 0 & 1 \\ 0 & 0 \end{bmatrix}\begin{bmatrix} x_1 \\ x_2 \end{bmatrix} + \begin{bmatrix} 0 & 0 \\ 0 & 1 \end{bmatrix}\begin{bmatrix} 0 \\ u(t) \end{bmatrix} \tag{36}$$

or

$$\frac{\mathrm{d}}{\mathrm{d}t}\begin{bmatrix} x_1 \\ x_2 \end{bmatrix} = \begin{bmatrix} 0 & 1 \\ 0 & 0 \end{bmatrix}\begin{bmatrix} x_1 \\ x_2 \end{bmatrix} + \begin{bmatrix} 0 \\ 1 \end{bmatrix} u(t), \tag{37}$$

where the state variables are the position $x_1$ and the velocity $x_2$. The model governed by Eq. (1) leads to

$$\mathbf{F} = \begin{bmatrix} 0 & 1 \\ 0 & 0 \end{bmatrix}, \quad \mathbf{H} = [1 \quad 0]$$

and these signals satisfy the following:

$$E[\mathbf{u}(t)\mathbf{u}^{\mathrm{T}}(\tau)] = \mathbf{Q}\delta(t-\tau), \quad E[\mathbf{v}(t)\mathbf{v}^{\mathrm{T}}(\tau)] = \mathbf{R}\delta(t-\tau), \quad E[\mathbf{u}(t)\mathbf{v}^{\mathrm{T}}(\tau)] = \mathbf{0}.$$

Expressing the models in discrete-time equivalent form, the corresponding $\mathbf{\Phi}_k$, $\mathbf{Q}_k$ and $\mathbf{H}$ are given by

$$\mathbf{\Phi}_k = \begin{bmatrix} 1 & \Delta t \\ 0 & 1 \end{bmatrix}. \tag{38}$$

(1) Approach 1

The matrices for representing Eq. (36) or (37), can be either of the following forms

$$\mathbf{G} = \begin{bmatrix} 0 & 0 \\ 0 & 1 \end{bmatrix}, \quad \mathbf{Q} = \begin{bmatrix} 0 & 0 \\ 0 & q \end{bmatrix}, \quad \mathbf{u}(t) = \begin{bmatrix} 0 \\ u(t) \end{bmatrix} \quad \text{(form 1)} \tag{39}$$

or

$$\mathbf{G} = \begin{bmatrix} 0 \\ 1 \end{bmatrix}, \quad \mathbf{Q} = q, \quad \mathbf{u}(t) = u(t) \quad \text{(form 2)}, \tag{40}$$

where the scalar $u(t) \sim N(0,q)$. It should be noted that given a matrix $\mathbf{G}$ with dimension $m \times n$, $\mathbf{Q}$ is a square matrix with dimension $n \times n$ and $\mathbf{GQG}^{\mathrm{T}}$ has dimension $m \times m$. As was mentioned earlier, the term $\mathbf{GQG}^{\mathrm{T}}$ describes the noise input and for this example

$$\mathbf{GQG}^{\mathrm{T}} = \begin{bmatrix} 0 & 0 \\ 0 & q \end{bmatrix}.$$

Calculation of covariance through Eq. (26) yields

$$\mathbf{\Gamma}_k \mathbf{Q}_k \mathbf{\Gamma}_k^{\mathrm{T}} = E[\mathbf{w}_k \mathbf{w}_k^{\mathrm{T}}] = \int_{t_k}^{t_{k+1}} \mathbf{\Phi}(t_{k+1}, \eta)\mathbf{GQG}^{\mathrm{T}}\mathbf{\Phi}^{\mathrm{T}}(t_{k+1}, \eta)\,\mathrm{d}\eta$$

$$= \begin{cases} \int_{t_k}^{t_k} \begin{bmatrix} 1 & \eta \\ 0 & 1 \end{bmatrix}\begin{bmatrix} 0 & 0 \\ 0 & 1 \end{bmatrix}\begin{bmatrix} 0 & 0 \\ 0 & q \end{bmatrix}\begin{bmatrix} 0 & 0 \\ 0 & 1 \end{bmatrix}\begin{bmatrix} 1 & 0 \\ \eta & 1 \end{bmatrix}\mathrm{d}\eta \quad \text{(via form 1)} \\ \int_{t_k}^{t_{k+1}} \begin{bmatrix} 1 & \eta \\ 0 & 1 \end{bmatrix}\begin{bmatrix} 0 \\ 1 \end{bmatrix} q [0 \quad 1] \begin{bmatrix} 1 & 0 \\ \eta & 1 \end{bmatrix}\mathrm{d}\eta \quad \text{(via form 2)} \end{cases} = \begin{bmatrix} \frac{\Delta t^3}{3} & \frac{\Delta t^2}{2} \\ \frac{\Delta t^2}{2} & \Delta t \end{bmatrix} q \tag{41}$$

(2) Approach 2
Calculation of noise gain through Eq. (30) yields

$$\mathbf{\Gamma}_k = \int_{t_k}^{t_{k+1}} \mathbf{\Phi}_k \mathbf{G}\, \mathrm{d}\tau = \int_{t_k}^{t_{k+1}} \begin{bmatrix} 1 & \tau \\ 0 & 1 \end{bmatrix} \begin{bmatrix} 0 \\ 1 \end{bmatrix} \mathrm{d}\tau = \begin{bmatrix} \frac{\Delta t^2}{2} \\ \Delta t \end{bmatrix}.$$

This result can be interpreted as follows. Given the $w_k$ to be the acceleration during the kth sampling period (of length $\Delta t$), in the increment in the velocity during this period is $w_k \Delta t$, while the effect of this (piecewise) constant acceleration on the position is $\frac{\Delta t^2}{2} w_k$, where the scalar $w_k \sim N(0, \sigma_w^2)$ is the noise variance of the random acceleration. Performing the $\mathbf{\Gamma}_k \mathbf{Q}_k \mathbf{\Gamma}_k^{\mathrm{T}}$ calculation gives

$$\mathbf{\Gamma}_k \mathbf{Q}_k \mathbf{\Gamma}_k^{\mathrm{T}} = \begin{bmatrix} \frac{\Delta t^2}{2} \\ \Delta t \end{bmatrix} \sigma_w^2 \begin{bmatrix} \frac{\Delta t^2}{2} & \Delta t \end{bmatrix} = \begin{bmatrix} \frac{\Delta t^4}{4} & \frac{\Delta t^3}{2} \\ \frac{\Delta t^3}{2} & \Delta t^2 \end{bmatrix} \sigma_w^2 \approx \begin{bmatrix} \frac{\Delta t^3}{4} & \frac{\Delta t^2}{2} \\ \frac{\Delta t^2}{2} & \Delta t \end{bmatrix} q. \tag{42}$$

In the present example, the relation holds true:

$$\mathbf{Q}_k \approx \frac{\mathbf{Q}}{\Delta t} = \sigma_w^2 = \frac{q}{\Delta t} \tag{43}$$

since $\mathbf{Q} = q$. The difference between Eqs. (40) and (42) should be mentioned. Both models are approximations. The advantage from Approach 2 is that the process noise intensity is easily related to physical characteristics of the motion, while Approach 1 is more convenient when one deal with variable sampling intervals [2].

## 4. Simulation of the dynamic process

In the subsequent discussion, three methods are presented for simulation of the dynamic process. The first two are base on the assumption of deterministic inputs while the third one is based on the random inputs.

### 4.1. Fundamental basis

#### 4.1.1. Numerical integration for the system states of equations

If the forcing function $\mathbf{u}$ is regarded as constant (i.e., a deterministic input) during the sampling period $\Delta t (= t_{k+1} - t_k)$, then $\mathbf{\Gamma}_k$ in the discrete-time form can be determined, and the numerical integration approach can be used. By use of the forward Euler approximation technique, we have

$$\dot{x}(t_k) \approx \frac{x(t_{k+1}) - x(t_k)}{t_{k+1} - t_k},$$

where $x(t_k)$ is though of as the sampled data value of the continuous-time signal $x(t)$. Substituting the above equation into the continuous-time state model results in

$$\frac{\mathbf{x}(t_{k+1}) - \mathbf{x}(t_k)}{t_{k+1} - t_k} \approx \mathbf{F}(t_k)\mathbf{x}(t_k) + \mathbf{G}(t_k)\mathbf{u}(t_k).$$

Consequently, the discrete-time model can be written in the form

$$\mathbf{x}(t_{k+1}) \approx [\mathbf{I} + \Delta t \mathbf{F}(t_k)]\mathbf{x}(t_k) + \Delta t \mathbf{G}(t_k)\mathbf{u}(t_k). \tag{44}$$

When compared to Eq. (11b), the matrix $\mathbf{\Phi}_k$ can be written as

$$\mathbf{\Phi}_k = \mathbf{I} + \mathbf{F}(t_k)\Delta t + \mathrm{O}(\Delta t^2) \tag{45}$$

and the gain matrix $\mathbf{\Gamma}_k$ as

$$\mathbf{\Gamma}_k = \mathbf{G}(t_k)\Delta t + \mathrm{O}(\Delta t^2). \tag{46}$$

Eqs. (45) and (46) are the first-order approximations of Eqs. (24) and (31), respectively.

*4.1.2. Numerical integration applied to each of the states*

For some of the large systems where calculation of $\mathbf{\Phi}_k$ and $\mathbf{\Gamma}_k$ are not preferable, performing the numerical integration for each of the states is another good choice. The initial-value problem described by the first-order ordinary differential equation:

$$\frac{\mathrm{d}\mathbf{x}}{\mathrm{d}t} = f(\mathbf{x}, t) \quad \text{subject to } \mathbf{x}(t_0) = \mathbf{x}_0$$

can be solved by employing the Euler's method:

$$\mathbf{x}_{k+1} \approx \mathbf{x}_k + \Delta t f(\mathbf{x}_k, t_k) = \mathbf{x}_k + \Delta t \dot{\mathbf{x}}_k \tag{47}$$

which is obtained by employing the forward difference approximation.

(3) Decomposition of the noise covariance matrix

If $\mathbf{Q}_k$ is symmetric and positive, it is possible to obtain a lower triangular matrix $\mathbf{C}$ through the *Cholesky factorization*

$$\mathbf{C}\mathbf{C}^{\mathrm{T}} = \mathbf{Q}_k \tag{48}$$

and

$$\mathbf{x}_{k+1} = \mathbf{\Phi}_k \mathbf{x}_k + \mathbf{C} \cdot \mathrm{randn} \cdot \left.\begin{bmatrix} 1 \\ \vdots \\ 1 \end{bmatrix}\right\} n \times 1, \tag{49}$$

where $\mathbf{x}_k$ is an $n \times 1$ matrix and randn stands for the unity Gaussian white sequence. It should be mentioned that singularity should be avoided when Eq. (49) is used. The process noise covariance matrix using Approach 2 (the direct discrete time models) are positive semidefinite of rank 1, while the one using Approach 1 (from the discretized continuous time models) are of full rank.

*4.2. Illustrative example*

Based on the three methods discussed in Part A, the example in Section 3 will be employed for illustration.

*4.2.1. Numerical integration for the system states of equations*

$$\mathbf{x}_{k+1} = \mathbf{\Phi}_k \mathbf{x}_k + \sigma_w \cdot \mathrm{randn} \cdot \mathbf{\Gamma}_k$$

for which the process noise matrix is represented by $\sigma_w \cdot \mathrm{randn} \cdot \mathbf{\Gamma}_k$.

$$x_1(k+1) = x_1(k) + x_2(k) \cdot \Delta t \left( + \sigma_w \cdot \mathrm{randn} \cdot \frac{\Delta t^2}{2} \right),$$

$$x_2(k+1) = x_2(k) + \sigma_w \cdot \mathrm{randn} \cdot \Delta t.$$

When the second-order term is included, then the noise gain $\mathbf{\Gamma}_k = \left[\frac{\Delta t^2}{2} \;\; \Delta t\right]^{\mathrm{T}}$, and the second order term (shown inside the bracket) is included; while when the first-order approximation is used, the noise gain becomes $\mathbf{\Gamma}_k = [0 \, \Delta t]^{\mathrm{T}}$, and the term in the bracket is neglected.

*4.2.2. Numerical integration applied to each of the states*

$$x_2(k+1) = x_2(k) + \sigma_w \cdot \mathrm{randn} \cdot \Delta t,$$

$$x_1(k+1) = x_1(k) + x_2(k+1) \cdot \Delta t,$$

where $\sigma_w \approx \sqrt{\frac{q}{\Delta t}}$.

The results are essentially same those obtained in Part (1) when the noise gain is obtained using the first-order approximation. The other distinction is that $x_2$ is calculated before $x_1$ is. This is to reflect the fact that $x_2$ is the derivative of $x_1$ and such arrangement provides latest $x_2$ information for performing $x_1$ calculation.

*4.2.3. Decomposition of the noise covariance matrix using the Cholesky factorization*

$$\mathbf{x}_{k+1} = \mathbf{\Phi}_k \mathbf{x}_k + \mathbf{C} \cdot \text{randn} \cdot \begin{bmatrix} 1 \\ 1 \end{bmatrix},$$
$$\begin{bmatrix} c_{11} & 0 \\ c_{21} & c_{22} \end{bmatrix} \begin{bmatrix} c_{11} & c_{21} \\ 0 & c_{22} \end{bmatrix} = \begin{bmatrix} q_{11} & q_{12} \\ q_{12} & q_{22} \end{bmatrix}$$

or

$$\begin{bmatrix} c_{11}^2 & c_{11}c_{21} \\ c_{11}c_{21} & c_{21}^2 + c_{22}^2 \end{bmatrix} = \begin{bmatrix} q_{11} & q_{12} \\ q_{12} & q_{22} \end{bmatrix},$$
$$c_{11} = \sqrt{q_{11}}, \quad c_{21} = \frac{q_{12}}{\sqrt{q_{11}}}, \quad c_{22} = \sqrt{q_{22} - \frac{q_{12}^2}{q_{11}}}.$$

The singularity problem addressed in Section 3 is demonstrated. Follow up the same example, decomposition of $\mathbf{\Gamma}_k \mathbf{Q}_k \mathbf{\Gamma}_k^{\mathrm{T}}$ for the results from the two approaches gives

– Approach 1:

$$\mathbf{\Gamma}_k \mathbf{Q}_k \mathbf{\Gamma}_k^{\mathrm{T}} = \begin{bmatrix} \frac{\Delta t^3}{3} & \frac{\Delta t^2}{2} \\ \frac{\Delta t^2}{2} & \Delta t \end{bmatrix} q$$

leads to

$$\mathbf{C} = \begin{bmatrix} \sqrt{\frac{\Delta t^3}{3}} & 0 \\ \frac{\sqrt{3}\Delta t}{2} & \frac{\sqrt{\Delta t}}{2} \end{bmatrix} \sqrt{q}$$

which is of full rank.

– Approach 2:

$$\mathbf{\Gamma}_k \mathbf{Q}_k \mathbf{\Gamma}_k^{\mathrm{T}} = \begin{bmatrix} \frac{\Delta t^4}{4} & \frac{\Delta t^3}{2} \\ \frac{\Delta t^3}{2} & \Delta t^2 \end{bmatrix} \sigma_w^2 \approx \begin{bmatrix} \frac{\Delta t^3}{4} & \frac{\Delta t^2}{2} \\ \frac{\Delta t^2}{2} & \Delta t \end{bmatrix} q$$

leads to

$$\mathbf{C} = \begin{bmatrix} \frac{\sqrt{\Delta t^3}}{2} & 0 \\ \sqrt{\Delta t} & 0 \end{bmatrix} \sqrt{q}$$

which is of positive semidefinite of rank 1.

## 5. Relation to the continuous Kalman filtering

The correctness of solutions obtained by the DTKF can be checked with those by the CKF. The main reason for choosing the CKF as a comparison basis is due to the fact that CKF solutions can be obtained without complicated computation and with better confidence on the correctness of solutions. In the following discussion, the results based on the DTKF for $\Delta t \to 0$ and $k \to \infty$ will be compared to the steady-state continuous Kalman filter (SSCKF). The SSCKF uses gains derived from the steady-state covariance and provides sub-optimal solutions. Expanding Eq. (7) leads to

$$\begin{aligned} \dot{P}_{11} &= 2P_{12} - \frac{1}{r}P_{11}^2, \\ \dot{P}_{12} &= P_{22} - \frac{1}{r}P_{11}P_{12}, \\ \dot{P}_{22} &= q - \frac{1}{r}P_{12}^2. \end{aligned} \tag{50}$$

The time varying error covariance and Kalman gain matrix can be obtained using the numerical integration such as the Euler or the Runge-Kutta integrator. When the system reaches the steady-state, we have

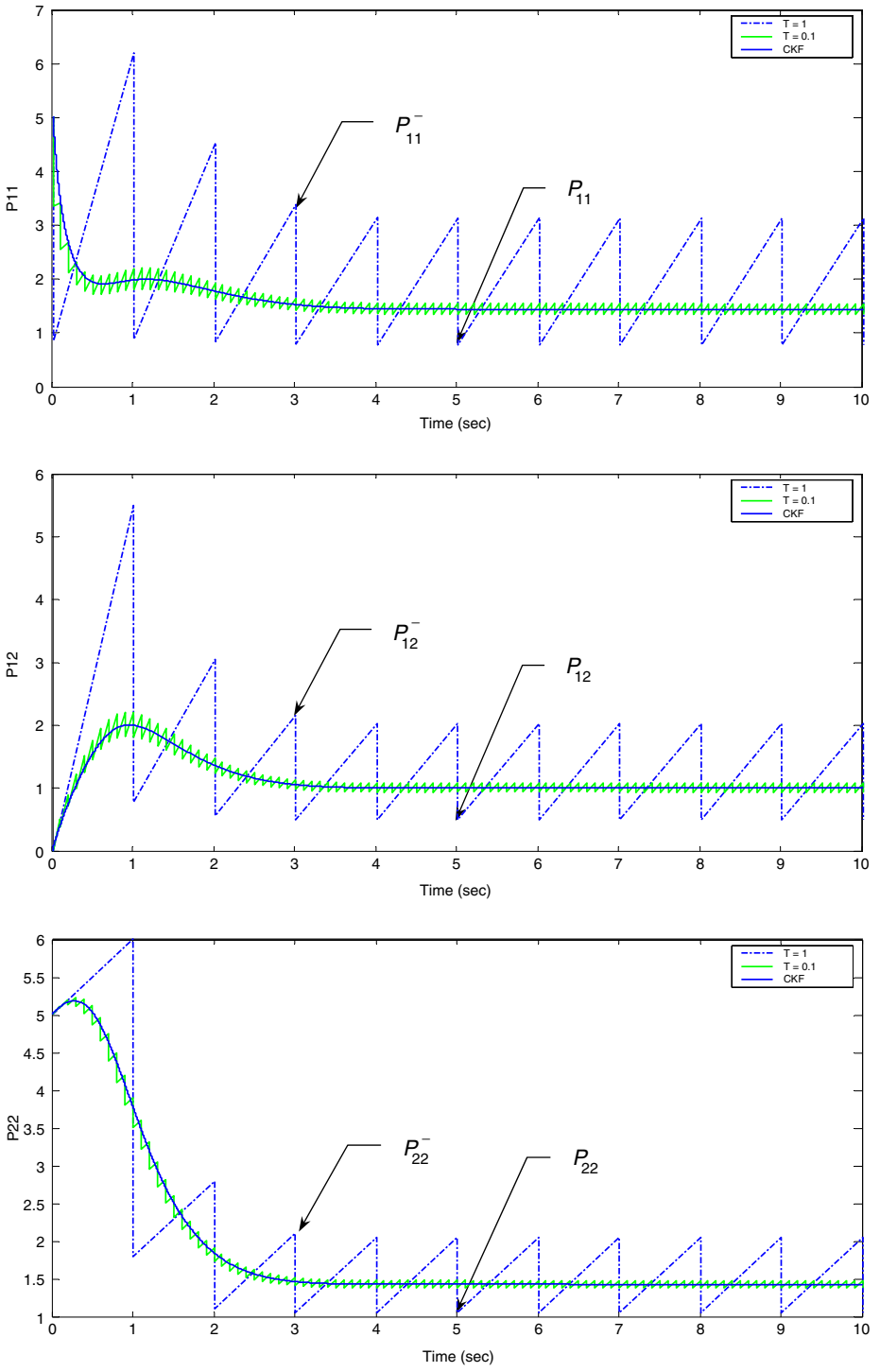


Fig. 1. Covariance propagation for the discrete time Kalman filter as compared to the continuous time Kalman filter.

$$\mathbf{P}_\infty = \begin{bmatrix} \sqrt{2}q^{1/4}r^{3/4} & (qr)^{1/2} \\ (qr)^{1/2} & \sqrt{2}q^{3/4}r^{1/4} \end{bmatrix}, \quad \mathbf{K}_\infty = \begin{bmatrix} \sqrt{2}\left(\frac{q}{r}\right)^{1/4} \\ \left(\frac{q}{r}\right)^{1/2} \end{bmatrix}.$$

For the present example, choosing $q = r = 1$ gives

$$\mathbf{P}_\infty = \begin{bmatrix} \sqrt{2} & 1 \\ 1 & \sqrt{2} \end{bmatrix}, \quad \mathbf{K}_\infty = \begin{bmatrix} \sqrt{2} \\ 1 \end{bmatrix}.$$

Fig. 1 shows the covariance propagation for the DTKF, for the cases of sampling period $\Delta t = 1$ and $\Delta t = 0.1$, as compared to the CKF.

Checking the numerical values when the simulation time is 10 s (for which it is a reasonable assumption that the system has reached steady-state), the predicted covariance (a priori), updated covariance (a posteriori) and Kalman gain matrices, respectively, are obtained as follows:

(1) For $\Delta t = 1$ s

$$\mathbf{P}^-_{k\to\infty} = \begin{bmatrix} 3.11 & 2.03 \\ 2.03 & 2.03 \end{bmatrix}, \quad \mathbf{P}_{k\to\infty} = \begin{bmatrix} 0.76 & 0.49 \\ 0.49 & 1.03 \end{bmatrix}, \quad \mathbf{K}_{k\to\infty} = \begin{bmatrix} 0.757 \\ 0.493 \end{bmatrix}.$$

(2) For $\Delta t = 0.1$ s

$$\mathbf{P}^-_{k\to\infty} = \begin{bmatrix} 1.52 & 1.07 \\ 1.07 & 1.47 \end{bmatrix}, \quad \mathbf{P}_{k\to\infty} = \begin{bmatrix} 1.32 & 0.93 \\ 0.93 & 1.36 \end{bmatrix}, \quad \mathbf{K}_{k\to\infty} = \begin{bmatrix} 0.132 \\ 0.093 \end{bmatrix}.$$

(3) For $\Delta t = 0.01$ s

$$\mathbf{P}^-_{k\to\infty} = \begin{bmatrix} 1.42 & 1.01 \\ 1.01 & 1.42 \end{bmatrix}, \quad \mathbf{P}_{k\to\infty} = \begin{bmatrix} 1.40 & 1 \\ 1 & 1.41 \end{bmatrix}, \quad \mathbf{K}_{k\to\infty} = \begin{bmatrix} 0.014 \\ 0.010 \end{bmatrix}.$$

Fig. 2 provides the filter gains for the case $\Delta t = 0.01$. Checking the values between the continuous filter gains $\mathbf{K}_\infty$ and discrete filter gains $\mathbf{K}_{k\to\infty}$ when the sampling time is small, e.g., $\Delta t = 0.01$ s is employed, it is seen that

$$\mathbf{K}_\infty \Delta t = 0.01 \begin{bmatrix} \sqrt{2} \\ 1 \end{bmatrix} \to \mathbf{K}_{k\to\infty}.$$

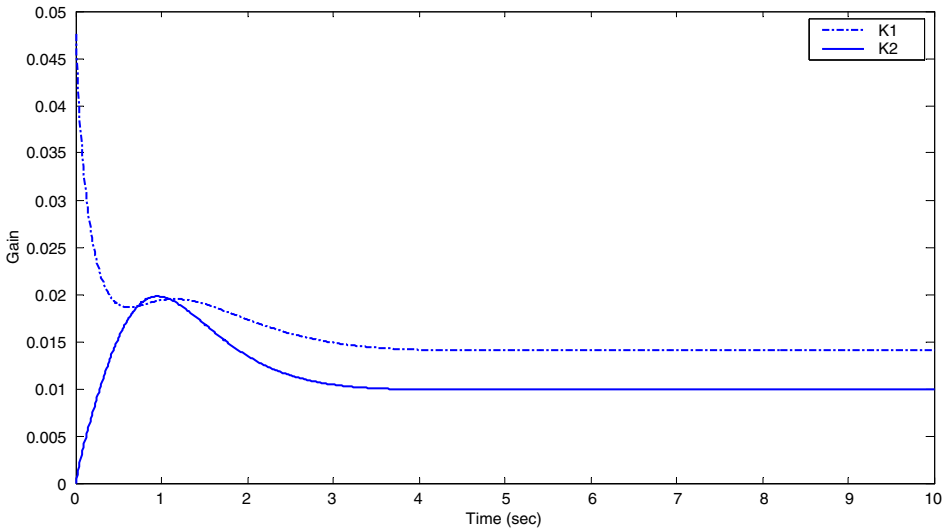


Fig. 2. Filter gains for the case of sampling period $\Delta t = 0.01$.

## 6. Estimator optimality evaluation with sensitivity analysis and consistency check

In this section, verification of minimum variance optimality with sensitivity analysis and consistency check for the Kalman filter is presented.

### 6.1. Estimator optimality evaluation with sensitivity analysis

#### 6.1.1. Theoretical error covariance check

The error covariance relationships for a discrete filter with the same structure as the Kalman filter, but with an arbitrary gain matrix are written as

$$\mathbf{P}_k = (\mathbf{I} - \mathbf{K}_k\mathbf{H}_k)\mathbf{P}_k^-(\mathbf{I} - \mathbf{K}_k\mathbf{H}_k)^{\mathrm{T}} + \mathbf{K}_k\mathbf{R}_k\mathbf{K}_k^{\mathrm{T}}, \tag{51}$$

$$\mathbf{P}_{k+1}^- = \mathbf{\Phi}_k\mathbf{P}_k\mathbf{\Phi}_k^{\mathrm{T}} + \mathbf{Q}_k \tag{17a}$$

or, if Eq. (11b) is used,

$$\mathbf{P}_{k+1}^- = \mathbf{\Phi}_k\mathbf{P}_k\mathbf{\Phi}_k^{\mathrm{T}} + \mathbf{\Gamma}_k\mathbf{Q}_k\mathbf{\Gamma}_k^{\mathrm{T}}. \tag{17b}$$

The error covariance $\mathbf{P}_k$ described in a single differential Eq. is obtained by substituting Eq. (17a) into Eq. (51):

$$\mathbf{P}_k = (\mathbf{\Phi}_k - \mathbf{K}_k\mathbf{H}_k\mathbf{\Phi}_k)\mathbf{P}_k(\mathbf{\Phi}_k - \mathbf{K}_k\mathbf{H}_k\mathbf{\Phi}_k)^{\mathrm{T}} + (\mathbf{I} - \mathbf{K}_k\mathbf{H}_k)\mathbf{Q}_k(\mathbf{I} - \mathbf{K}_k\mathbf{H}_k)^{\mathrm{T}} + \mathbf{K}_k\mathbf{R}_k\mathbf{K}_k^{\mathrm{T}} \tag{52}$$

which has an equivalent form in the CKF:

$$\dot{\mathbf{P}} = (\mathbf{F} - \mathbf{K}\mathbf{H})\mathbf{P} + \mathbf{P}(\mathbf{F} - \mathbf{K}\mathbf{H})^{\mathrm{T}} + \mathbf{G}\mathbf{Q}\mathbf{G}^{\mathrm{T}} + \mathbf{K}\mathbf{R}\mathbf{K}^{\mathrm{T}}. \tag{53}$$

In view of CKF, Eq. (53) defines the error covariance for the filter with a general filter gain matrix $\mathbf{K}$, which can be solved for the covariance of an arbitrary gain model. The sensitivity analysis can be conveniently implemented by using such representation. Taking the partial derivative of $\mathbf{P}_\infty$ with respect to $\mathbf{K}$, using $\frac{\partial \mathbf{P}_\infty}{\partial \mathbf{K}} = 0$ for a minimum leads to the same result as Eq. (7).

If the fixed-gain matrix $\mathbf{K}$ of a filter has been designed for particular values of $\mathbf{Q}$ and $\mathbf{R}$, the steady-state error covariance will vary linearly with the actual process noise spectral density or measurement error spectral density. If the actual noise variances are assumed fixed and the design values of $\mathbf{Q}$ and $\mathbf{R}$ are varied, significantly different curves result. Any deviation of the design variances, and consequently $\mathbf{K}$, from the correct values will cause an increase in the filter error variance (a consequence of the optimality of the filter). Further information on sensitivity analysis can be referred to Gelb [4].

The error covariance for the filter with the arbitrary gain model, can be obtained using Eq. (53):

$$\begin{aligned}
\dot{P}_{11} &= -2K_1P_{11} + 2P_{12} + K_1^2 r,\\
\dot{P}_{12} &= \dot{P}_{21} = -K_2P_{11} - K_1P_{12} + P_{22} + K_1K_2 r,\\
\dot{P}_{22} &= -2K_2P_{12} + K_2^2 r + q.
\end{aligned} \tag{54}$$

The covariances are influenced by (1) the actual noise strength (PSD's) in the external environment; (2) the gain matrix (which can be any gain matrix and not necessarily the Kalman gain matrix). If the gain matrix is the Kalman gain matrix, the above equations leads to Eq. (50) and the optimal result with minimum variance will be obtained. By setting $\dot{\mathbf{P}} = \mathbf{0}$, the solutions related to arbitrary gains are found to be

$$\begin{bmatrix} P_{11\infty} & P_{12\infty} \\ P_{12\infty} & P_{22\infty} \end{bmatrix} = \frac{1}{2K_{1\infty}K_{2\infty}} \begin{bmatrix} q + K_{1\infty}^2K_{2\infty}r + K_{2\infty}^2 r & (q + K_{2\infty}^2 r)K_{1\infty} \\ (q + K_{2\infty}^2 r)K_{1\infty} & K_{1\infty}^2 q + K_{2\infty}q + K_{2\infty}^3 r \end{bmatrix}. \tag{55}$$

The results demonstrate the influence of the (steady-state) gain deviation on the variance growth.

For the standard Kalman filter, the filter gain $\mathbf{K}_k$ minimizes the following performance index:

$$J = \mathrm{tr}(E[\mathbf{e}\mathbf{e}^{\mathrm{T}}]) = \mathrm{tr}(\mathbf{P}), \tag{56}$$

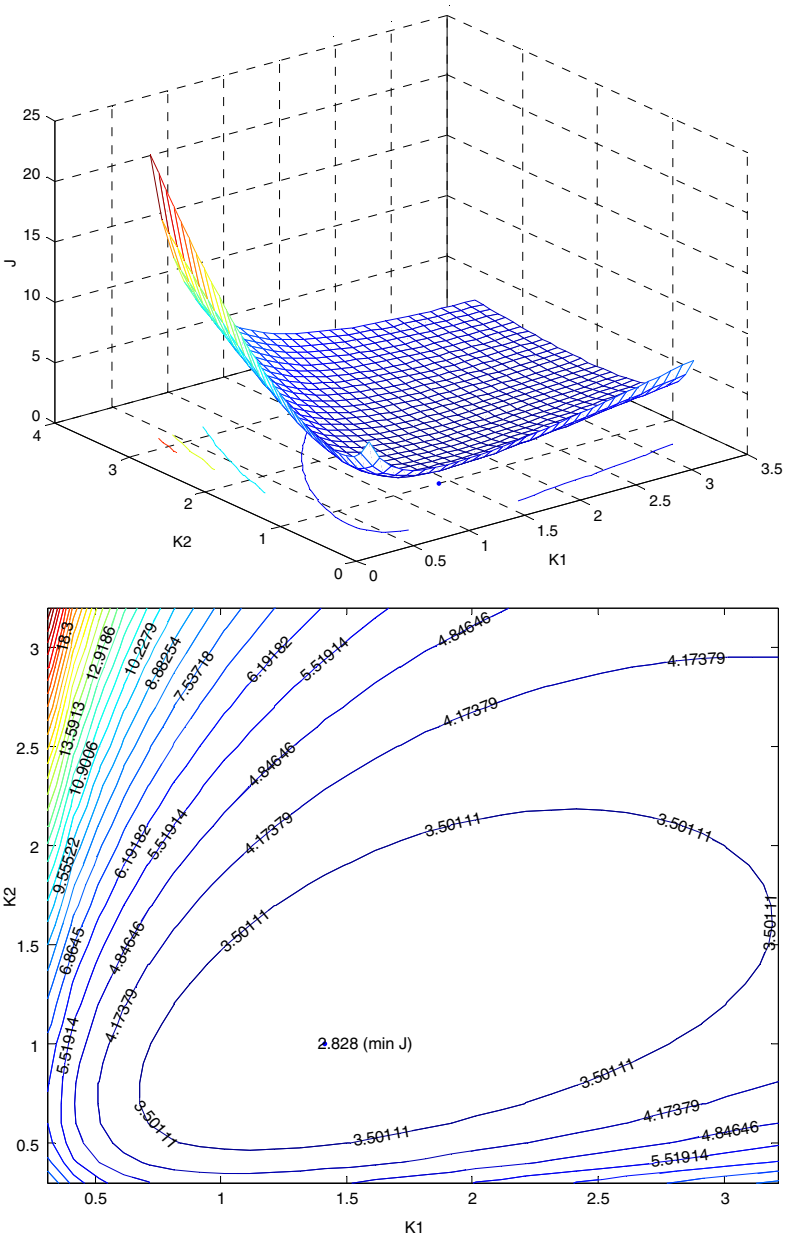


Fig. 3. 3-D plot for the cost function (top), and the corresponding contour plot (bottom), for $q = r = 1$.

where tr(·) denotes the trace of a matrix and **P** is obtained using Eq. (55). If there is no uncertainty in the process and measurement noise covariances the performance index $J$ attains the global minimum using the standard Kalman filter. However, in the case that there are uncertainties in $\mathbf{Q}_k$ or $\mathbf{R}_k$, $J$ would not attain the minimum. Fig. 3 shows the 3-D plot for the cost function, and the corresponding contour plot for $q = r = 1$.

*6.1.2. Theoretical versus simulated error covariances*

To perform statistical analysis of the system actual performance in comparison with the filter estimate of its statistical performance, the theoretical (predicted) covariance is compared to the simulated (actual) covariance. Continued from the preceding example for illustration, Fig. 4 demonstrates (1) the influence of position variance and velocity variance due to $K_1$ deviation from the optimal point; (2) influence of position variance

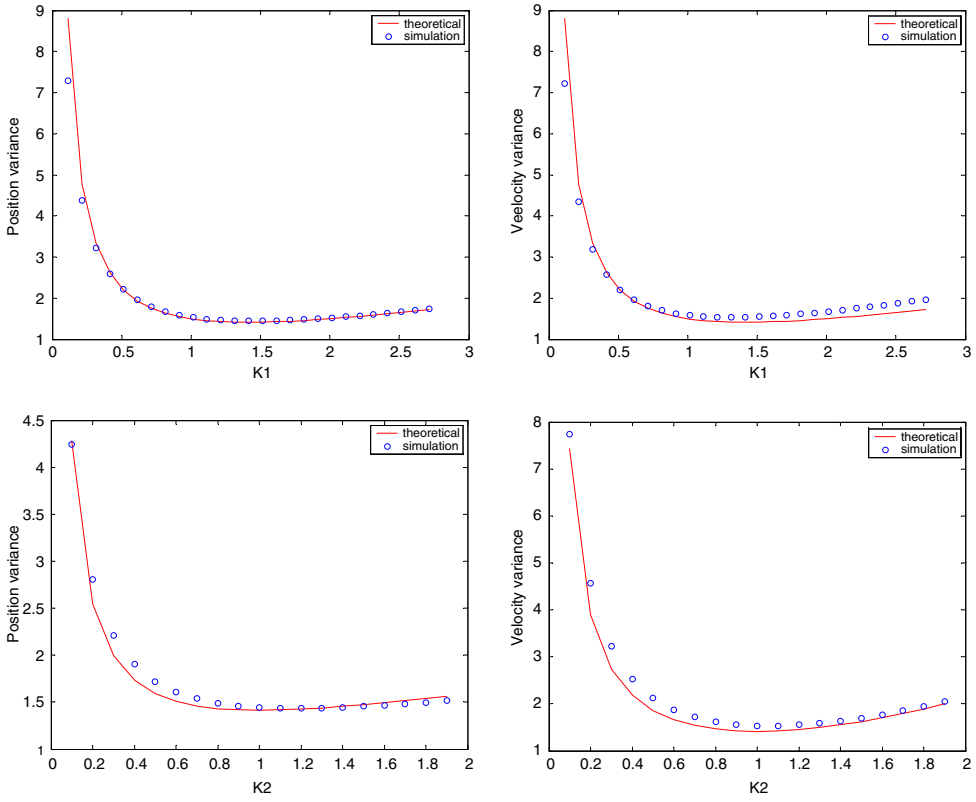


Fig. 4. Influence of position variance (top left) and velocity variance (top right) due to $K_1$ deviation from the optimal point; influence of position variance (bottom left) and velocity variance (bottom left) due to $K_2$ deviation from the optimal point.

and velocity variance due to $K_2$ deviation from the optimal point. Results represented by solid lines show the theoretical prediction results (from Eq. (55)) while results denoted by circles show the statistics based on numerical simulation results for the collected data.

$$\mathrm{MSE} = \frac{1}{N}\sum(\hat{\mathbf{x}} - \mathbf{x}_{\mathrm{true}})^2,$$

where $N$ is the number of samples. Such offline single run (simulation) test is based on replacing the ensemble averages by time averages based on the ergodicity assumption. It is seen that the theoretical prediction and numerical simulation results are in very close agreement.

### 6.2. Consistency check between theoretical and simulation results

In addition to optimality check, consistency check for the optimality should be conducted. Since the filter gain is based on the filter-calculated error covariances, it follows that consistency is necessary for filter optimality. Not all filter divergence is predictable from the Riccati equation solution. Sometimes the actual performance does not agree with theoretical performance. One cannot measure estimation error directly, except in simulations, therefore it is necessary to find other means to check on estimation accuracy. Whenever the estimation error is deemed to differ significantly from its expected value as computed by the Riccati equation, the filter is said to diverge from its predicted performance.

The results were verified using multiple simulations (runs). Fig. 5 shows the 100 ensembles and the one sigma $(1-\sigma)$ confidence bound. Data were collected from the 100 simulation runs. Total time for each simulation run is set to be 10 s with $\Delta t = 0.1$ s, which leads to 101 samples per run, and totally gives 10100 samples for the entire 100 runs. For this example, the mean and variance are computed to be $m_x = 0.24$ (ideally to be

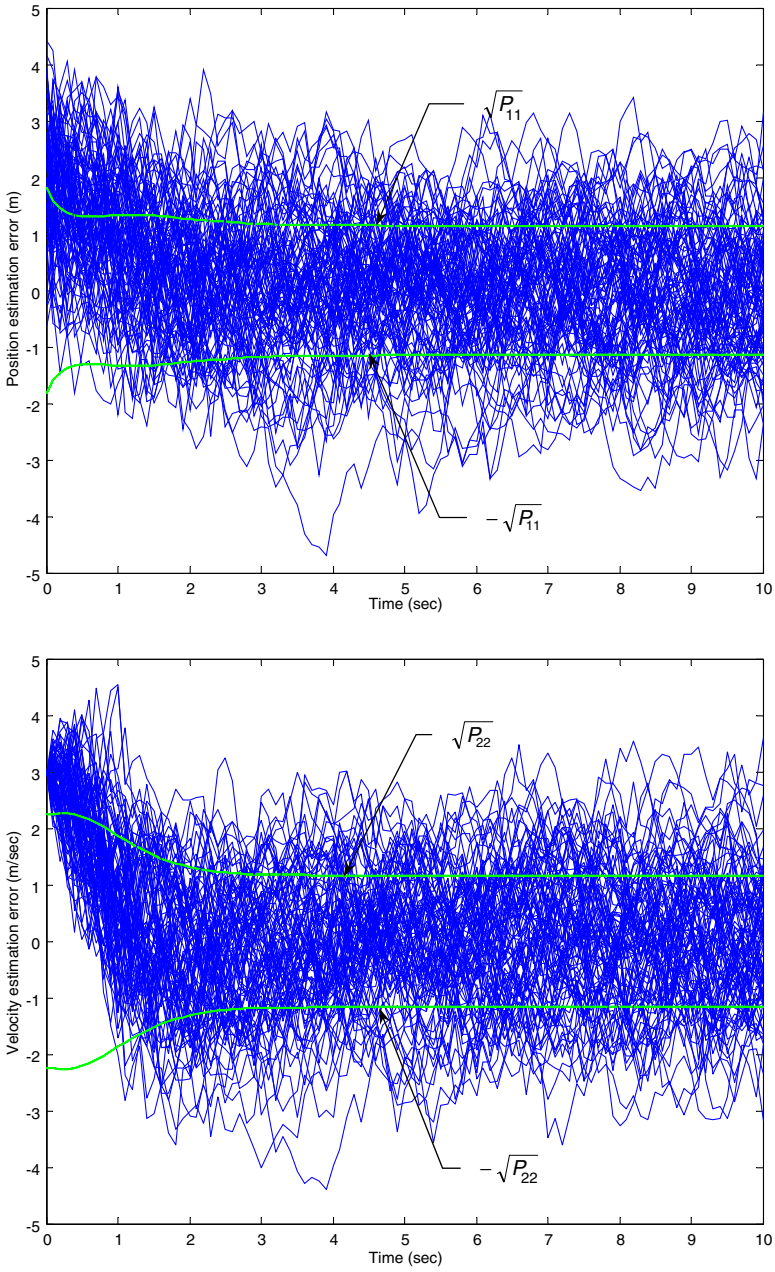


Fig. 5. Ensemble of the filtering estimation errors based on 100 runs: position (top) and velocity (bottom) component.

zero for an unbiased estimator); $\sigma = 1.22$ (compared to the theoretical prediction to be 1.32 as obtained in Section 5). Histograms of the position estimation error are obtained and compared to the theoretical one. The theoretical probability density function (PDF) of the position estimation error are obtained by substituting the calculated mean and variance into the Gaussian (normal) PDF given by

$$f_X(x) = \frac{1}{\sqrt{2\pi}\sigma} \exp\left[-\frac{1}{2\sigma^2}(x - m_x)^2\right].$$

Theoretical and histograms of the position estimation error are shown as in Fig. 6. Both approaches are in very good agreement.

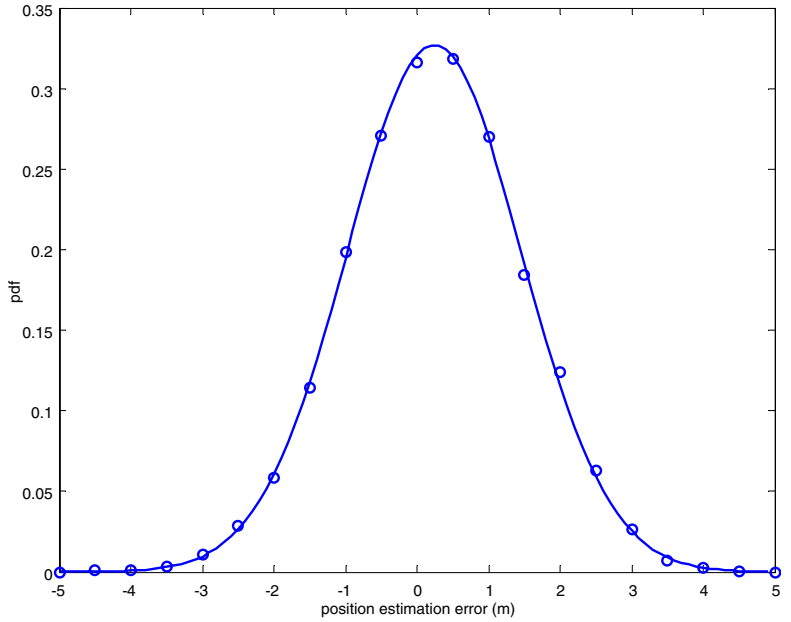


Fig. 6. Theoretical and histograms of the position estimation error.

## 7. Conclusions

This paper has discussed several remarks which are useful for the designers in understanding, simulating and verifying the Kalman filter computer codes. A tutorial, example-based approach is employed to present several KF issues of considerable importance in engineering practice, and to suggest some check points on Kalman filtering verification process. Lessons learned from this paper include: (1) Additional notes on two forms of the discrete-time Kalman filter loop; (2) Methods for determining of the process noise covariance matrix; (3) Simulation of the dynamic process; (4) Consistency verification for the discrete-time Kalman filter as compared to the continuous Kalman filtering; (5) Evaluation of estimator optimality for verification of minimum variance optimality with sensitivity analysis (of the error growth due to incorrect estimate of the noise), as well as the consistency check between theoretical and simulation results.

## Acknowledgement

The authors gratefully acknowledge the support of the National Science Council of the Republic of China through Grant NSC 93-2212-E-019-004 and NSC 94-2212-E-019-003.

## References

[1] Y. Bar-Shalom, X.R. Li, T. Kirubarajan, Estimation with Applications to Tracking and Navigation, John Wiley & Sons, Inc., 2001.
[2] K. Brammer, G. Karlsruhe, Kalman-Bucy Filters, Artech House, 1988.
[3] R. Brown, P. Hwang, Introduction to Random Signals and Applied Kalman Filtering, John Wiley & Sons, New York, 1997.
[4] A. Gelb, Applied Optimal Estimation, M.I.T. Press, MA, 1974.
[5] M.S. Grewal, A.P. Andrews, Kalman Filtering, Theory and Practice Using MATLAB, second ed., John Wiley & Sons, Inc., 2001.
[6] F.L. Lewis, Optimal Estimation, John Wiley & Sons, Inc., 1986.